

Communication: Energetics of reaction pathways for reactions of ethenol with the hydroxyl radical: The importance of internal hydrogen bonding at the transition state

Oksana Tishchenko, Sonia Ilieva, and Donald G. Truhlar^{a)}

Department of Chemistry and Supercomputing Institute, University of Minnesota, Minneapolis, Minnesota 55455-0431, USA

(Received 12 April 2010; accepted 1 June 2010; published online 14 July 2010)

We find high multireference character for abstraction of H from the OH group of ethenol (also called vinyl alcohol); therefore we adopt a multireference approach to calculate barrier heights for the various possible reaction channels of OH+C₂H₃OH. The relative barrier heights of ten possible saddle points for reaction of OH with ethenol are predicted by multireference Møller–Plesset perturbation theory with active spaces based on correlated participating orbitals (CPOs) and CPO plus a correlated π orbital (CPO+ π). Six barrier heights for abstracting H from a C—H bond range from 3.1 to 7.7 kcal/mol, two barrier heights for abstracting H from an O—H bond are both 6.0 kcal/mol, and two barrier heights for OH addition to the double bond are -1.8 and -2.8 kcal/mol. Thus we expect abstraction at high-temperature and addition at low temperature. The factor that determines which H is most favorable to abstract is an internal hydrogen bond that constitutes part of a six-membered ring at one of the abstraction saddle points; the hydrogen bond contributes about 3 kcal/mol stabilization. © 2010 American Institute of Physics. [doi:10.1063/1.3455996]

One of the challenges of modeling combustion and atmospheric chemistry is determining the reaction rates of intermediate species because their kinetics is often difficult to study directly. Quantum chemistry is playing an increasingly important role in this process. Enols have been implicated as intermediates in combustion,^{1–4} and they may play a role in atmospheric chemistry,⁵ but little is known about their reactions with hydroxyl radical, which is the most important oxidizing species in both environments. Here we compute the barrier heights for the possible reactions of ethenol with hydroxyl radical.

Preliminary calculations using several single-reference methods showed energy convergence problems for abstraction of H from the OH-group. Therefore, the calculations of the barrier heights and all geometry optimizations were carried out using multireference Møller–Plesset second order perturbation theory^{6,7} (MRMP2) based on complete active space self-consistent-field^{8–11} (CASSCF) (also known as the fully optimized reaction space^{12,13}) reference wave functions. With few exceptions,^{14,15} the MRMP2 method has not been systematically applied for geometry optimization of reactive saddle points, but the application of this method to a single-point energy calculation at geometries optimized at a different level is more common.^{16–20} With both approaches, the resulting accuracy has been encouraging. The mean unsigned error in the exothermic-direction barrier heights calculated using the MRMP2/*nom*-CPO/*aug-cc-pVTZ* model chemistry for the reactions of the DBH24 database²¹ is 1.1 kcal/mol.¹⁴ The CASPT2 method^{22,23} (CAS stands for complete active space, and PT2 stands for second-order perturbation theory; CASPT2 is closely related to MRMP2) has also been used

successfully for barrier height calculations, again usually with CASSCF geometries. (Representative applications may be consulted for details.^{24–32}) Recently, calculations on the reactions of OH with propene were reported by Izsák *et al.*,³³ who employed CASPT2 geometry optimizations. Harding *et al.*^{34,35} have obtained good results with CASPT2-optimized transition states.

The possible reaction channels considered in this paper may be divided into three groups: (i) Abstraction from a C—H bond, (ii) abstraction from an O—H bond, and (iii) addition of the OH radical across the C=C bond to the α or β carbon of the ethenol. The active space in each case was constructed based on the correlating participating orbitals¹⁴ (CPOs) prescription. The active space used for (iii) is the nominal CPO (*nom*-CPO) defined previously,¹⁴ and the active spaces for two other reaction groups are the *nom*-CPO plus the pair of π and π^* orbitals of the double bond; this latter choice is denoted here as *nom*-CPO+ π .

The *nom*-CPO active space is designed¹⁴ to capture the major portion of nondynamical correlation for a particular reaction channel. The *nom*-CPO active space involves the bonding and antibonding combinations of the breaking and forming bonds and the singly occupied molecular orbital (SOMO) of a radical (the orbital which is singly occupied in its ground electronic state). We use the convention¹⁴ that a pipe between two orbitals indicates an orbital of the reactant (left) and the corresponding orbital of the product (right). With this notation, the active spaces used in the present calculations contain the $\sigma_{\text{CH}}|\sigma_{\text{OH}}$, $\sigma_{\text{CH}}^*|\sigma_{\text{OH}}^*$, π , π^* , and SOMO(O)|SOMO(C) orbitals for the C—H abstraction reactions, the $\sigma_{\text{OH}_{\text{ethenol}}}\sigma_{\text{OH}_{\text{water}}}$, $\sigma_{\text{OH}_{\text{ethenol}}}^*\sigma_{\text{OH}_{\text{water}}}^*$, π , π^* , and SOMO(O_{OH})|SOMO(O_{OCHCH₂}) orbitals for the O—H abstraction reaction, and $\pi_{\text{CC}}|\sigma_{\text{CO}}$, $\pi_{\text{CC}}^*|\sigma_{\text{CO}}^*$, and

^{a)}Electronic mail: truhlar@umn.edu.

TABLE I. Calculated barrier heights (using the MRMP2/nom-CPO+ π /aug-cc-pVTZ model chemistry, except where indicated otherwise; V_{syn} : Barrier for reaction of syn-ethenol relative to the OH+*syn*-ethenol asymptote; $V_{anti}-\Delta E_{syn-anti}$: Barrier for reaction of anti-ethenol relative to the OH+*anti*-ethenol asymptote; V_{anti} : Barrier for reaction of anti-ethenol relative to the OH+*syn*-ethenol asymptote. The values in the second last column are obtained by adding the M06/aug-cc-pVTZ *syn-anti* energy difference of 1.3 kcal/mol to the MRMP2/nom-CPO+ π /aug-cc-pVTZ value of the barrier with respect to OH+*anti*-ethenol asymptote.) and reaction energies (using G3SX/M05-2X/aug-cc-pVTZ, in kcal/mol) for reactions of ethenol with OH radical.

Reaction	Label ^a	V_{syn}	ΔE	Label ^a	$V_{anti}-\Delta E_{syn-anti}$	V_{anti}	ΔE
(C)H abstraction	s1	3.11	-4.5	s1a	5.39	6.7	-4.9
(C)H abstraction	s2	6.55	-6.0	s2a	6.40	7.7	-4.1
(C)H abstraction	s3	6.76	-10.1	s3a	4.42	5.7	-11.3
(O)H abstraction	s4	6.04 (5.50) ^b	-34.2	s4a	4.68	6.0	-34.4
C=C alpha addition	s5	-1.84	-31.9				
C=C beta addition	s6	-2.78	-33.2				

^aLabels are for corresponding saddle point geometries shown in Fig. 1.

^bThe value in parentheses is calculated using MRMP2/mod-CPO+ π /aug-cc-pVTZ. The mod-CPO active space is constructed by adding to the nom-CPO active space the unshared pairs in *p* orbitals geminal to bonds that are broken or formed (Ref. 14).

SOMO(O)|SOMO(C) pairs of orbitals for addition reactions. The active space for the abstraction reaction channels thus corresponds to five electrons in five orbitals, and the active space for the addition reactions corresponds to three electrons in three orbitals.

All calculations employed the aug-cc-pVTZ basis set.³⁶ All calculations of the barrier heights were performed using the GAMESS suite of programs.³⁷ Additionally, reaction energies have been calculated by single point energy evaluations using the G3SX (Ref. 38) method at geometries optimized using the M05-2X (Ref. 39) density functional. These calculations have been performed with the GAUSSIAN⁴⁰ code.

Ethenol can exist in two conformers: *syn* and *anti*. We used the M06 density functional⁴¹ with the aug-cc-pVTZ basis set to calculate that the *anti* conformer is 1.3 kcal/mol higher than *syn*, and the *syn-to-anti* barrier is 5.3 kcal/mol (and therefore the *anti-to-syn* barrier is 4.0 kcal/mol). Using MRMP2 as explained above, we found eight saddle points for abstraction reactions and two for addition reactions.⁴² The classical barrier heights with respect to reactants (OH + H₂C=CHOH) are given in Table I. For *syn*-ethenol these were obtained by comparing the saddle point energy to the energy of a *syn*-reactant. For *anti*-ethenol they were obtained by comparing the saddle point energy to the energy of an *anti*-reactant, and adding the *anti-syn* energy difference. The optimized geometries are given in tabular form in supplementary material⁴³ and are displayed in Fig. 1. Geometries of reactants were fully optimized in the supermolecule approach, with the distance separating the reactants fixed at least at 25 Å. For each possible reaction, the reactants have been optimized separately to preserve the invariance of the orbital active space.

The invariance of the orbital active space implies that the active orbitals gradually transform from the reactant region to the product region of a potential energy and therefore cause no discontinuities on the global potential energy surface. This requirement, however, may result in an unbalanced treatment of products versus transition state structures for highly exothermic reactions (or reactants versus transition state structures for highly endothermic reactions), if the

number of the orbitals in an active space is relatively small. This happens because the active space selected using the CPO prescription does not necessarily include the most correlated orbitals for a reactant (or product) structure if such a structure is considerably lower in energy than the transition state. For example, in the case of very exothermic addition reactions of ozone to π systems, the bond-making π -type orbital of the reactant transforms into a lower-lying σ -type (C—O) orbital of the product, which is not the best candidate for an active space of the product structure if the latter were considered on its own. Therefore, the forward barrier heights for these reactions have been found to be more accurate than the reverse ones.⁴⁴ Here, for that reason, since all of the reactions are exothermic and some are highly exothermic, we present only forward barrier heights.

When OH approaches ethenol there is a complex at an energy 4.4 kcal/mol lower than the separated *syn*-ethenol and OH, as calculated by MRMP2. After that there are barriers to α and β addition but they are below the reactant asymptote. The barriers to H abstraction are positive though, and the lowest of them equals 3.1 kcal/mol. Therefore we expect the dominant reactions to be α and β addition at low temperatures and H abstraction at high temperatures.

The key geometrical parameters of the optimized saddle point structures are shown in Fig. 1. The geometries in Fig. 1 explain why **s1** has a considerably lower energy than the other abstraction saddle points; in particular, **s1** shows an internal hydrogen bond as part of a six-membered ring (present at the transition state and the complex, but not for reactants and not for the other seven of the eight transition states), and Table I shows that this stabilizes the **s1** saddle point by about 3 kcal/mol. Other examples of stabilizing abstraction transition states by five- and six-membered ring hydrogen bonds are available for comparison.⁴⁵ Although the hydrogen bonding lowers the energy of one of the transition states, it also probably raises its zero point energy and lowers its entropy because the vibrational frequencies will be higher at the tighter transition state; both of those effects will partly or fully compensate the favorable energetic effect of the hydrogen bonding. One must consider zero point vibrational

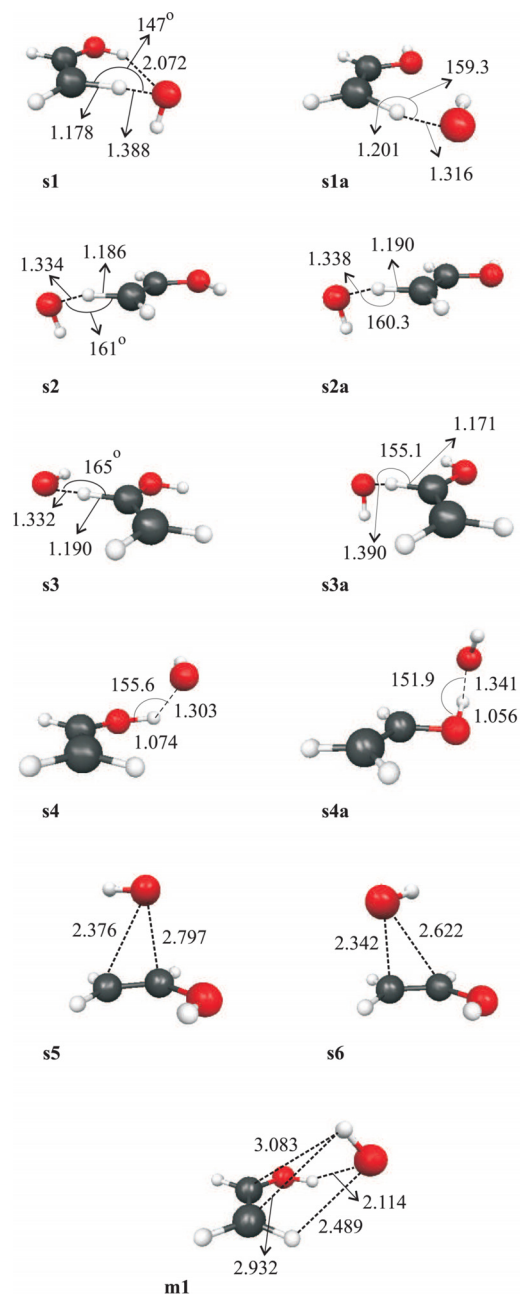


FIG. 1. Key geometrical parameters (distances in angstroms, angles in degrees) of the reactive saddle points (**s1**–**s6**, **s1a**–**s4a**) and the reactant complex (**m1**) for reactions of ethenol with the hydroxyl radical. All structures are optimized using the MRMP2/nom-CPO+ π /aug-cc-pVTZ model chemistry.

energy and vibrational-rotational thermal energy and entropy as well as electronic energy in estimating the free energy of activation for passing through a transition state or generalized transition state, and a reliable calculation of these effects will require treating vibrational anharmonicity as well.⁴⁶

Correlations^{47,48} between geometric and energetic features, e.g., the correlations implied by the Hammond postulate,⁴⁹ can be found for the reaction channels (of the same group) that do not involve formation of the hydrogen bond. For example, when considering the **s2**, **s3**, **s2a**, and **s3a** transition state structures in terms of the O \cdots H and the C \cdots H distances and the corresponding barrier heights, one can see that the lowest barrier in the case of **s3a** corresponds to the earliest transition structure and the highest barrier in case of **s3** corresponds to the latest transition structure.

Additional calculations on the reaction channel (ii) have been performed by employing the MRMP2/mod-CPO+ π /aug-cc-pVTZ model chemistry. The difference between the nom-CPO and mod-CPO active spaces is that the latter also includes the unshared electron pairs in *p* orbitals geminal to bonds that are broken or formed,¹⁴ in the present case, the unshared electron pairs in *p* orbitals of the oxygen atoms. The difference of about 0.5 kcal/mol between the barrier heights calculated by applying the MRMP2/nom-CPO+ π /aug-cc-pVTZ and MRMP2/mod-CPO+ π /aug-cc-pVTZ model chemistries is within the uncertainty¹⁴ of the methods. One may anticipate that the effect of the larger active space would even be smaller in the cases of the reaction channels (i) and (iii) because only one oxygen atom involved in the bond breaking-bond making process in these cases.

It is interesting to ask whether a multireference approach was essential for this reaction. To examine this question, we computed the *M* diagnostic¹⁴ for each saddle point. The *M* diagnostic is defined in terms of the eigenvalues of the single-particle density matrix of the CASSCF wave function, and we found that $M > 0.04$ often signals significant errors in calculated barrier heights if single-reference methods are applied.¹⁴ Table II shows that $M = 0.050$ – 0.055 for the reactants and reactive saddle points in the present article. In all cases the *M* diagnostic is dominated by the static correlation of the π bond, and this does not change appreciably from case to case; hence *M* is not larger for **s4** and **s4a** than for the other structures. On the basis of the convergence problems with the single-reference wave functions and the large *M* values we concluded that multireference methods are essen-

TABLE II. Multireference diagnostics for reactions of ethenol with OH radical (*M* is defined in Ref. 14).

Reaction	Label ^a	<i>M</i>		<i>M</i>		
		Saddle point	Reactants	Saddle point	Reactants	
(C)H abstraction	s1	0.050	0.050	s1a	0.055	0.053
(C)H abstraction	s2	0.052	0.050	s2a	0.054	0.052
(C)H abstraction	s3	0.052	0.051	s3a	0.053	0.053
(O)H abstraction	s4	0.052	0.052	s4a	0.055	0.054
C=C alpha addition	s5	0.052	0.052			
C=C beta addition	s6	0.055	0.052			

^aLabels are for corresponding saddle point geometries shown in Fig. 1.

tial for comparing the various saddle point energies in a balanced way. The MRMP2 method has performed well in previous tests for barrier heights,^{14,15,17,19,44} and this gives added confidence in the reliability of the present results.

This work was supported in part by the U.S. Department of Energy, Office of Basic Energy Sciences under Grant No. DE-F602-86ER13579. This research used resources of the Argonne Leadership Computing Facility at Argonne National Laboratory, which is supported by the Office of Science of the U.S. Department of Energy under Contract DE-AC02-06CH11357 and resources of Minnesota Supercomputing Institute of the University of Minnesota.

- ¹C. A. Taatjes, N. Hansen, A. Mclroy, J. A. Miller, J. P. Senosiain, S. J. Klippenstein, F. Qi, L. Sheng, Y. Zhang, T. A. Cool, J. Wang, P. R. Westmoreland, M. E. Law, T. Kasper, and K. Kohse-Höinghaus, *Science* **308**, 1887 (2005).
- ²C. A. Taatjes, N. Hansen, J. A. Miller, T. A. Cool, J. Wang, P. R. Westmoreland, M. E. Law, T. Kasper, and K. Kohse-Höinghaus, *J. Phys. Chem. A* **110**, 3254 (2006).
- ³H. R. Zhang, L. K. Huynh, N. Kungwan, S. Zhang, Z. Yang, T. Truong, E. Eddings, and A. Sarofim, *Prepr. Pap. - Am. Chem. Soc., Div. Fuel Chem.* **51**, 229 (2006).
- ⁴G. da Silva, C.-H. Kim, and J. W. Bozzelli, *J. Phys. Chem. A* **110**, 7925 (2006).
- ⁵M. Ganot, Y. Yair, C. Price, B. Ziv, Y. Sherez, E. Greenberg, A. Devir, and R. Yaniv, *Geophys. Res. Lett.* **34**, L12801 (2007).
- ⁶K. Hirao, *Chem. Phys. Lett.* **190**, 374 (1992).
- ⁷K. Hirao, *Int. J. Quantum Chem., Quantum Chem. Symp.* **44**, 517 (1992).
- ⁸B. O. Roos, P. R. Taylor, and P. E. M. Siegbahn, *Chem. Phys.* **48**, 157 (1980).
- ⁹P. E. M. Siegbahn, J. Almlöf, A. Heiberg, and B. O. Roos, *J. Chem. Phys.* **74**, 2384 (1981).
- ¹⁰H.-J. Werner and P. J. Knowles, *J. Chem. Phys.* **82**, 5053 (1985); P. J. Knowles and H.-J. Werner, *Chem. Phys. Lett.* **115**, 259 (1985).
- ¹¹B. O. Roos, *Adv. Chem. Phys.* **69**, 399 (1987).
- ¹²L. M. Cheung, K. R. Sundberg, and K. Ruedenberg, *Int. J. Quantum Chem.* **16**, 1103 (1979); K. Ruedenberg, M. W. Schmidt, M. M. Gilbert, and S. T. Elbert, *Chem. Phys.* **71**, 41 (1982).
- ¹³M. W. Schmidt and M. S. Gordon, *Annu. Rev. Phys. Chem.* **49**, 233 (1998).
- ¹⁴O. Tishchenko, J. J. Zheng, and D. G. Truhlar, *J. Chem. Theory Comput.* **4**, 1208 (2008).
- ¹⁵B. A. Ellingson, D. P. Theis, O. Tishchenko, J. Zheng, and D. G. Truhlar, *J. Phys. Chem. A* **111**, 13554 (2007).
- ¹⁶O. Roberto-Neto, F. B. Machado, and D. G. Truhlar, *J. Chem. Phys.* **111**, 10046 (1999).
- ¹⁷Y. Kobayashi, M. Kamiya, and K. Hirao, *Chem. Phys. Lett.* **319**, 695 (2000).
- ¹⁸O. Tishchenko, E. S. Kryachko, C. Vinckier, and M. T. Nguyen, *Chem. Phys. Lett.* **363**, 550 (2002).
- ¹⁹O. Tishchenko, C. Vinckier, and M. T. Nguyen, *J. Phys. Chem. A* **108**, 1268 (2004).
- ²⁰O. Tishchenko, C. Vinckier, A. Ceulemans, and M. T. Nguyen, *J. Phys. Chem. A* **109**, 6099 (2005).
- ²¹J. Zheng, Y. Zhao, and D. G. Truhlar, *J. Chem. Theory Comput.* **3**, 569 (2007).
- ²²K. Andersson, P.-A. Malmqvist, and B. O. Roos, *J. Chem. Phys.* **96**, 1218 (1992).
- ²³H.-J. Werner, *Mol. Phys.* **89**, 645 (1996); P. Celani and H.-J. Werner, *J. Chem. Phys.* **112**, 5546 (2000).
- ²⁴N. Marchand, P. Jimeno, J. C. Rayez, and D. Liotard, *J. Phys. Chem.* **101**, 6077 (1997).
- ²⁵P. R. Schreiner, *J. Am. Chem. Soc.* **120**, 4184 (1998).
- ²⁶M. T. Nguyen, A. K. Chandra, S. Sakai, and K. Morokuma, *J. Org. Chem.* **64**, 65 (1999).
- ²⁷P. N. Skancke, D. A. Hrovat, and W. T. Borden, *J. Phys. Chem. A* **103**, 4043 (1999).
- ²⁸F. Sevin and M. L. McKee, *J. Am. Chem. Soc.* **123**, 4591 (2001).
- ²⁹W. T. G. Johnson, M. B. Sullivan, and C. J. Cramer, *Int. J. Quantum Chem.* **85**, 492 (2001).
- ³⁰A. G. Leach and K. N. Houk, *Org. Biomol. Chem.* **1**, 1389 (2003).
- ³¹V. Guner, K. S. Khuong, A. G. Leach, P. S. Lee, M. D. Bartberger, and K. N. Houk, *J. Phys. Chem.* **107**, 11445 (2003).
- ³²W. H. Lam, P. P. Gaspar, D. A. Hrovat, D. A. Trieber II, E. R. Davidson, and W. T. Borden, *J. Am. Chem. Soc.* **127**, 9886 (2005).
- ³³R. Izsák, M. Szori, P. J. Knowles, and B. Viskolcz, *J. Chem. Theory Comput.* **5**, 2313 (2009).
- ³⁴L. B. Harding, S. J. Klippenstein, and A. W. Jasper, *Phys. Chem. Chem. Phys.* **9**, 4055 (2007).
- ³⁵L. B. Harding, S. J. Klippenstein, and J. A. Miller, *J. Phys. Chem.* **112**, 522 (2008).
- ³⁶R. A. Kendall, T. H. Dunning, Jr., and R. J. Harrison, *J. Chem. Phys.* **96**, 6796 (1992).
- ³⁷M. W. Schmidt, K. K. Baldrige, J. A. Boatz, S. T. Elbert, M. S. Gordon, J. H. Jensen, S. Koseki, N. Matsunaga, K. A. Nguyen, S. J. Su, T. L. Windus, M. Dupuis, and J. A. Montgomery, *J. Comput. Chem.* **14**, 1347 (1993).
- ³⁸L. A. Curtiss, P. C. Redfern, and K. Raghavachari, *J. Chem. Phys.* **114**, 108 (2001).
- ³⁹Y. Zhao, N. E. Schultz, and D. G. Truhlar, *J. Chem. Theory Comput.* **2**, 364 (2006).
- ⁴⁰M. J. Frisch, G. W. Trucks, H. G. Schlegel *et al.*, GAUSSIAN 03, Revision C.01, Gaussian, Inc., Pittsburgh, PA, 1998.
- ⁴¹Y. Zhao and D. G. Truhlar, *Theor. Chem. Acc.* **120**, 215 (2008).
- ⁴²T. H. Dunning, Jr., *J. Chem. Phys.* **90**, 1007 (1989).
- ⁴³See supplementary material at <http://dx.doi.org/10.1063/1.3455996> for geometries of all optimized structures.
- ⁴⁴Y. Zhao, O. Tishchenko, J. R. Gour, W. Lei, J. J. Lutz, P. Piecuch, and D. G. Truhlar, *J. Phys. Chem. A* **113**, 5786 (2009).
- ⁴⁵R. Zhu and M. C. Lin, *PhysChemComm* **4**, 106 (2001); M. Liessmann, B. Hansmann, P. G. Blachly, J. S. Francisco, and B. Abel, *J. Phys. Chem.* **113**, 7570 (2009); J. S. Francisco and W. Eisfeld, *ibid.* **113**, 7593 (2009).
- ⁴⁶B. A. Fernandez-Ramos, in *Reviews in Computational Chemistry*, edited by K. B. Lipkowitz and T. R. Cundari (Wiley-VCH, Hoboken, 2007), Vol. 23, pp. 125–232.
- ⁴⁷M. H. Mok and J. C. Polanyi, *J. Chem. Phys.* **51**, 1451 (1969).
- ⁴⁸C. A. Parr and D. G. Truhlar, *J. Phys. Chem.* **75**, 1844 (1971).
- ⁴⁹G. S. Hammond, *J. Am. Chem. Soc.* **77**, 334 (1955).